SINGULARLY PERTURBED SYSTEMS

Many models of dynamic systems contain small parameters multiplying some of the time derivatives. When such small parameters are neglected, the dynamic order of the model is usually reduced, as illustrated by the series *RLC* circuit

$$LC\ddot{v} + RC\dot{v} + v = u \tag{1}$$

in Fig. 1, where v is the capacitor voltage and u is the applied voltage. If the inductance L is very small, then it is common

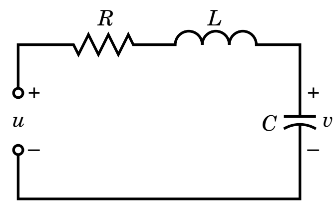

Figure 1. *RLC* circuit.

to neglect it and replace the second-order *RLC* equation (1) by the first-order *RC* equation

$$RC\dot{\bar{v}} + \bar{v} = u \tag{2}$$

in Fig. 2. Neglecting several such "parasitic" parameters (small time constants, masses, moments of inertia, etc.) often leads to a significant simplification of a high-order model. To validate such simplifications, we must examine whether, and in what sense, a lower-order model approximates the main phenomenon described by the original high-order model.

To see the issues involved, consider the *RLC* circuit in Eq. (1) with $u = 0$. Its free transients are due to the amount of energy stored in C and L, that is, the initial conditions $v(0)$ and $\dot{v}(0)$, respectively. The simplified model in Eq. (2) disregards the transient due to $\dot{v}(0)$, that is, the dissipation of energy stored in the inductance L. When L is small, this transient is fast, and after a short initial time, the *RC* equation (2) provides an adequate description of the remaining slow transient due to the energy stored in C.

The *RLC* circuit in Eq. (1) with a small L is a two-time-scale system, and the *RC* circuit in Eq. (2) is its slow time-scale approximation. In higher-order models, several small parameters may cause a multi-time-scale phenomenon, which can be approximated by "nested" two-time-scale models. In this article we consider only the two-time-scale systems.

In this example, a parameter perturbation from $L > 0$ to $L = 0$ has resulted in a model order reduction. Such parameter perturbations are called singular, as opposed to regular perturbations, which do not change the model order. For example, if instead of L, the small parameter is R, then its perturbation from $R > 0$ to $R = 0$ leaves the order of the *RLC* equation (1) unchanged. The resulting undamped sinusoidal oscillation is due to both $v(0)$ and $\dot{v}(0)$.

In the engineering literature of the past 30 years, singular perturbation techniques and their applications have been discussed in hundreds of papers and a dozen of books. This article presents only the basic singular perturbation tools for reduced-order modeling and systematic approximation of two-time-scale systems. Our main sources are the textbook by Kokotovic, Khalil, and O'Reilly (1) and the IEEE collection of

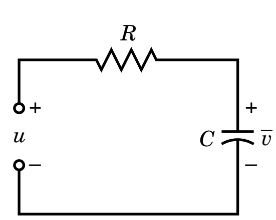

Figure 2. *RC* circuit.

benchmark papers edited by Kokotovic and Khalil (2). These books and the references therein are recommended for further reading.

TIME-SCALE PROPERTIES OF THE STANDARD MODEL

Several examples in the next section will show that a common state-space model of many two-time-scale systems is

$$\dot{x} = f(x, z, \epsilon, t), \quad x(t_0) = x_0 \tag{3a}$$

$$\epsilon\dot{z} = g(x, z, \epsilon, t), \quad z(t_0) = z_0 \tag{3b}$$

where $x \in R^{n_s}$, $z \in R^{n_f}$, and $\epsilon > 0$ is the small singular perturbation parameter. The parameter ϵ represents the small time constants and other "parasitics" to be neglected in the slow time-scale analysis.

The rate of change of z in Eq. (3b) is of order $1/\epsilon$, that is, $\dot{z} = O(1/\epsilon)$, which means that z exhibits a fast transient. When this fast transient settles, the longer-term behavior of x and z is determined by the quasi-steady-state equation

$$g(\bar{x}, \bar{z}, 0, t) = 0 \tag{4}$$

where the bar indicates that this equation is obtained by setting $\epsilon = 0$ in Eq. (3b). This equation will make sense only if it has one or several distinct ("isolated") roots

$$\bar{z} = \phi(\bar{x}, t) \tag{5}$$

for all $\bar{x}$ and $\bar{z}$ of interest. If this crucial requirement is satisfied, for example, when $\det(\partial g/\partial z) \neq 0$, then we say that system (3) is a standard model.

The substitution of Eq. (5) into Eq. (3a) results in the reduced model

$$\dot{\bar{x}} = f(\bar{x}, \phi(\bar{x}, t), 0, t), \quad \bar{x}(t_0) = x_0 \tag{6}$$

If Eq. (4) has several distinct roots as shown in Eq. (5), then each of them leads to a distinct reduced model as shown in Eq. (6). The singular perturbation analysis determines which of these models provides an $O(\epsilon)$ approximation of the slow phenomenon in system (3).

When, and in what sense, will $\bar{x}(t)$, $\bar{z}(t)$ obtained from Eqs. (6) and (5) be an approximation of the true solution of system (3)? To answer this question, we examine the variable z, which has been excluded from the reduced model in Eq. (6) by $\bar{z} = \phi(\bar{x}, t)$. In contrast to the original variable z, which starts at t_0 from a prescribed z_0, the quasi-steady state $\bar{z}$ is not free to start from a prescribed value, and there may be a large discrepancy between $\bar{z}(t_0) = \phi(x_0, t_0)$ and the prescribed initial state z_0. Thus, $\bar{z}(t)$ cannot be a uniform approximation of z. The best we can expect is that the approximation $z - \bar{z}(t) = O(\epsilon)$ will hold on an interval excluding t_0, that is, for $t \in [t_b, t_f]$ where $t_b > t_0$. On the other hand, it is reasonable to expect the approximation $x - \bar{x}(t) = O(\epsilon)$ to hold uniformly for all $t \in [t_0, t_f]$ because $x(t_0) = \bar{x}(t_0)$. If the error $z - \bar{z}(t)$ is indeed $O(\epsilon)$ over $[t_b, t_f]$, then it must be true that during the initial ("boundary-layer") interval $[t_0, t_b]$ the variable z approaches $\bar{z}$. Let us remember that the speed of z can be large since $\dot{z} = g/\epsilon$. In fact, having set $\epsilon = 0$ in Eq. (3b), we have made the transient of z instantaneous whenever $g \neq 0$. It is clear that we cannot expect z to converge to its quasi-steady state $\bar{z}$ unless certain stability conditions are satisfied.

To analyze the stability of the fast transient, we perform the change of variables $y = z - \phi(x, t)$, which shifts the quasi-steady state of z to the origin. Then Eq. (3b) becomes

$$\epsilon\dot{y} = g(x, y + \phi(x, t), \epsilon, t) - \epsilon\frac{\partial\phi}{\partial t} - \epsilon\frac{\partial\phi}{\partial x} f(x, y + \phi(x, t), \epsilon, t),$$
$$y(t_0) = z_0 - \phi(x_0, t_0) \tag{7}$$

Let us note that $\epsilon\dot{y}$ may remain finite even when ϵ tends to zero and $\dot{y}$ tends to infinity. We introduce a fast time variable τ by setting

$$\epsilon\frac{dy}{dt} = \frac{dy}{d\tau};\ \text{hence,}\ \frac{d\tau}{dt} = \frac{1}{\epsilon}$$

and use $\tau = 0$ as the initial value at $t = t_0$. The fast time variable $\tau = (t - t_0)/\epsilon$ is "stretched": if ϵ tends to zero, τ tends to infinity even for finite fixed t only slightly larger than t_0. In the τ scale, system (7) is represented by

$$\frac{dy}{d\tau} = g(x, y + \phi(x, t), \epsilon, t) - \epsilon\frac{\partial\phi}{\partial t} - \epsilon\frac{\partial\phi}{\partial x} f(x, y + \phi(x, t), \epsilon, t),$$
$$y(0) = z_0 - \phi(x_0, t_0) \tag{8}$$

In the fast time-scale τ, the variables t and x are slowly varying because $t = t_0 + \epsilon\tau$ and $x = x(t_0 + \epsilon\tau)$. Setting $\epsilon = 0$ freezes these variables at $t = t_0$ and $x = x_0$ and reduces Eq. (8) to the autonomous system

$$\frac{dy}{d\tau} = g(x_0, y + \phi(x_0, t_0), 0, t_0), \quad y(0) = z_0 - \phi(x_0, t_0) \tag{9}$$

which has equilibrium at $y = 0$. The frozen parameters (x_0, t_0) in Eq. (9) depend on the given initial state and initial time.

Tikhonov's Theorem

In our investigation of the stability of the origin of the system in Eq. (9), we should allow the frozen parameters to take any values in the domain of interest. Therefore, we rewrite the system in Eq. (9) as

$$\frac{dy}{d\tau} = g(x, y + \phi(x, t), 0, t) \tag{10}$$

where (x, t) are treated as fixed parameters. We refer to the system in Eq. (10) as the boundary-layer system and assume its exponential stability, uniform in the frozen parameters; that is,

$$\|y(\tau)\| \leq k\|y(0)\|e^{-\alpha\tau} \tag{11}$$

for some positive constants k and α. Furthermore, we assume that $y(0)$ belongs to the region of attraction of the origin. Under these conditions, a fundamental result of singular perturbation theory, called Tikhonov's Theorem, guarantees that the approximations

$$x = \bar{x}(t) + O(\epsilon) \tag{12a}$$

$$z = \phi(\bar{x}(t), t) + \hat{y}(t/\epsilon) + O(\epsilon) \tag{12b}$$

hold uniformly for $t \in [t_0, t_f]$, where $\hat{y}(\tau)$ is the solution of the system in Eq. (9). Moreover, given any $t_b > t_0$, the approximation

$$z = \phi(\bar{x}(t), t) + O(\epsilon) \tag{13}$$

holds uniformly for $t \in [t_b, t_f]$.

Local exponential stability of the boundary-layer system can be guaranteed with the eigenvalue condition

$$\text{Re}\left[\lambda\left\{\frac{\partial g}{\partial z}(x, \phi(x,t), 0, t)\right\}\right] \le -c < 0 \tag{14}$$

for all (x, t) in the domain of interest, where λ denotes the eigenvalues and c is a positive constant. Alternatively, it can be verified by a Lyapunov analysis if there is a Lyapunov function $W(x, y, t)$ that depends on (x, t) as parameters and satisfies

$$c_1\|y\|^2 \le W(x,y,t) \le c_2\|y\|^2 \tag{15}$$

$$\frac{\partial W}{\partial y} g(x, y + \phi(x,t), 0, t) \le -c_3\|y\|^2 \tag{16}$$

over the domain of interest, where c_1 to c_3 are positive constants independent of (x, t).

Slow Manifold

In the state-space $R^{n_s} \times R^{n_f}$ of (x, z), the equation $g(\bar{x}, \bar{z}, 0, t) = 0$ forces $\bar{x}$ and $\bar{z}$ to lie in an n_s-dimensional quasi-steady-state manifold $\overline{M}$, explicitly described by Eq. (5). It can be shown that, under the conditions of Tikhonov's Theorem, there exists an $\epsilon^* > 0$ such that for all $\epsilon \in (0, \epsilon^*]$, the system in Eq. (3) possesses an integral manifold M_ϵ that is invariant: whenever $x(t_0), z(t_0) \in M_\epsilon$, then $x(t), z(t) \in M_\epsilon$ for all $t \in [t_0, t_f]$. The *slow manifold* M_ϵ is in the ϵ-neighborhood of the quasi-steady-state manifold $\overline{M}$. We will characterize M_ϵ in the special case when f and g in the system in Eq. (3) do not depend on t and ϵ:

$$\dot{x} = f(x,z) \tag{17a}$$

$$\epsilon\dot{z} = g(x,z) \tag{17b}$$

A derivation of slow manifolds for systems with f and g also dependent on t and ϵ is given in Ref. (26).

We will seek the graph of M_ϵ in the explicit form $M_\epsilon : z = \phi(x, \epsilon)$. The existence of M_ϵ gives a clear geometric meaning to the slow subsystem of the full-order model in Eq. (17): it is the restriction of the model in Eq. (17) to the slow manifold M_ϵ, given by

$$\dot{x} = f(x, \phi(x, \epsilon)) \tag{18}$$

To find M_ϵ, we differentiate the manifold $z = \phi(x, \epsilon)$ with respect to t

$$\dot{z} = \frac{d}{dt}\phi(x,\epsilon) = \frac{\partial \phi}{\partial x}\dot{x} \tag{19}$$

and, upon the multiplication by ϵ and the substitution for $\dot{x}$ and $\dot{z}$, we obtain the *slow manifold condition*

$$\epsilon\frac{\partial \phi}{\partial x} f(x, \phi(x,\epsilon)) = g(x, \phi(x,\epsilon)) \tag{20}$$

which $\phi(x, \epsilon)$ must satisfy for all x of interest and all $\epsilon \in (0, \epsilon^*]$. This is a partial differential equation, which, in general, is difficult to solve. However, its solution can be approximated by the power series

$$\phi(x,\epsilon) = \varphi_0(x) + \epsilon\varphi_1(x) + \epsilon^2\varphi_2(x) + \cdots \tag{21}$$

where the functions $\varphi_0(x), \varphi_1(x), \ldots$, can be found by equating the terms with like powers in ϵ. To this end, we expand f and g as power series of ϵ

$$f(x, \varphi_0(x) + \epsilon\varphi_1(x) + \cdots) = f(x, \varphi_0(x)) + \epsilon\frac{\partial f}{\partial z}\varphi_1(x) + \cdots \tag{22}$$

$$g(x, \varphi_0(x) + \epsilon\varphi_1(x) + \cdots) = g(x, \varphi_0(x)) + \epsilon\frac{\partial g}{\partial z}\varphi_1(x) + \cdots \tag{23}$$

where all the partial derivatives are evaluated at x and $z = \varphi_0(x)$.

We substitute Eqs. (22) and (23) into Eq. (20). The terms with ϵ^0 yield

$$g(x, \varphi_0(x)) = 0, \text{ that is, } \phi(x,0) = \varphi_0(x) \tag{24}$$

which is the quasi-steady-state manifold $\overline{M}$. Equating the ϵ^1 terms, we get

$$\frac{\partial g}{\partial z}\varphi_1(x) = \frac{\partial \varphi_0(x)}{\partial x} f(x, \varphi_0(x)) \tag{25}$$

For the standard model, $\det(\partial g/\partial z) \neq 0$, that is, $\partial g/\partial z$ is nonsingular, so that

$$\varphi_1(x) = \left(\frac{\partial g}{\partial z}\right)^{-1}\frac{\partial \varphi_0(x)}{\partial x} f(x, \varphi_0(x)) \tag{26}$$

This recursive process can be repeated to find the higher-order terms in Eq. (21).

The fast off-manifold variable is

$$y = z - \phi(x,\epsilon) \tag{27}$$

In the x,y coordinates, the system in Eq. (17) becomes

$$\dot{x} = f(x, \phi(x,\epsilon) + y) \tag{28a}$$

$$\epsilon\dot{y} = g(x, \phi(x,\epsilon) + y) - \epsilon\frac{\partial \phi}{\partial x} f(x, \phi(x,\epsilon) + y) \tag{28b}$$

In these coordinates, the slow manifold M_ϵ is simply $y = 0$, that is, the equilibrium manifold of Eq. (28b). The geometry of a third-order system in Eq. (17) with $x \in R^2$ and $z \in R^1$ is illustrated in Fig. 3. Starting from an off-manifold initial con-

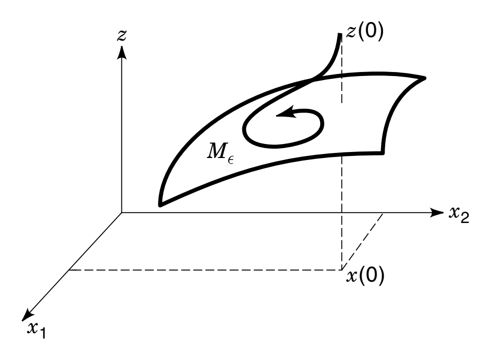

Figure 3. Trajectory converging to a slow manifold.

dition ($x(0)$, $z(0)$), the state trajectory rapidly converges to M_ϵ and then slowly evolves along M_ϵ.

Linear Two-Time-Scale Systems

The manifold condition in Eq. (20) is readily solvable for linear two-time-scale systems

$$\dot{x} = A_{11}x + A_{12}z + B_1u, \quad x(t_0) = x_0 \tag{29a}$$

$$\epsilon\dot{z} = A_{21}x + A_{22}z + B_2u, \quad z(t_0) = z_0 \tag{29b}$$

where A_{22} is nonsingular, which corresponds to $\det(\partial g/\partial z) \neq 0$, and $u \in R^m$ is the control input vector. The change of variables

$$y = z + L(\epsilon)x \tag{30}$$

where the $n_f \times n_s$ matrix $L(\epsilon)$ satisfies the matrix quadratic equation

$$A_{21} - A_{22}L + \epsilon LA_{11} - \epsilon LA_{12}L = 0 \tag{31}$$

transforms the system in Eq. (29) into a block-triangular system

$$\begin{bmatrix} \dot{x} \\ \epsilon\dot{y} \end{bmatrix} = \begin{bmatrix} A_{11} - A_{12}L & A_{12} \\ 0 & A_{22} + \epsilon LA_{12} \end{bmatrix} \begin{bmatrix} x \\ y \end{bmatrix} + \begin{bmatrix} B_1 \\ B_2 - \epsilon LB_1 \end{bmatrix} u \tag{32}$$

with the initial condition

$$\begin{bmatrix} x(t_0) \\ y(t_0) \end{bmatrix} = \begin{bmatrix} x_0 \\ z_0 + Lx_0 \end{bmatrix} \tag{33}$$

Note that Eq. (31) is the slow manifold condition in Eq. (20) for linear systems.

Given that A_{22} is nonsingular, the implicit function theorem implies that Eq. (31) admits a solution $L(\epsilon)$ for ϵ sufficiently small. Furthermore, an asymptotic expansion of the solution to Eq. (31) is given by

$$L(\epsilon) = A_{22}^{-1}A_{21} + \epsilon A_{22}^{-2}A_{21}(A_{11} - A_{12}A_{22}^{-1}A_{21}) + O(\epsilon^2) \tag{34}$$

We can readily verify that for $\epsilon = 0$, Eq. (31) reduces to

$$A_{21} - A_{22}L(0) = 0 \tag{35}$$

whose solution is the first term in Eq. (34). Furthermore, to solve for the higher-order terms, an iterative scheme

$$L_{k+1} = A_{22}^{-1}A_{21} + \epsilon A_{22}^{-1}L_k(A_{11} - A_{12}L_k), \quad L_0 = A_{22}^{-1}A_{21} \tag{36}$$

can be used.

Although the fast variable y in the triangular system in Eq. (32) is now decoupled from the slow variable x, the slow variable x is still driven by the fast variable y. To remove this influence, the change of variables

$$\xi = x - \epsilon H(\epsilon)y \tag{37}$$

where the $n_s \times n_f$ matrix $H(\epsilon)$ satisfies the linear matrix equation

$$\epsilon(A_{11} - A_{12}L)H - H(A_{22} + \epsilon LA_{12}) + A_{12} = 0 \tag{38}$$

applied to Eq. (32) results in the block-diagonal system

$$\begin{bmatrix} \dot{\xi} \\ \epsilon\dot{y} \end{bmatrix} = \begin{bmatrix} A_{11} - A_{12}L & 0 \\ 0 & A_{22} + \epsilon LA_{12} \end{bmatrix} \begin{bmatrix} \xi \\ y \end{bmatrix} + \begin{bmatrix} B_1 - H(B_2 + \epsilon LB_1) \\ B_2 - \epsilon LB_1 \end{bmatrix} u \tag{39}$$

with the initial condition

$$\begin{bmatrix} \xi(t_0) \\ y(t_0) \end{bmatrix} = \begin{bmatrix} x_0 - \epsilon H(z_0 + Lx_0) \\ z_0 + Lx_0 \end{bmatrix} \tag{40}$$

For ϵ sufficiently small, Eq. (38) admits a unique solution $H(\epsilon)$ that can be expressed as

$$H(\epsilon) = A_{12}A_{22}^{-1} + O(\epsilon) \tag{41}$$

The solution $H(\epsilon)$ can also be computed iteratively as

$$H_{k+1} = A_{12}A_{22}^{-1} + \epsilon((A_{11} - A_{12}L)H_k + H_kLA_{12})A_{22}^{-1}, \quad H_0 = A_{12}A_{22}^{-1} \tag{42}$$

If L is available from the recursive formula (36), we can use L_{k+1} instead of L in Eq. (42).

From the block-diagonal form in Eq. (39), it is clear that the slow subsystem of Eq. (29) is approximated to $O(\epsilon)$ by

$$\dot{\xi} = A_0\xi + B_0u, \quad \xi(t_0) = x_0 \tag{43}$$

where $A_0 = A_{11} - A_{12}A_{22}^{-1}A_{21}$ and $B_0 = B_1 - A_{12}A_{22}^{-1}B_2$. The fast subsystem is approximated to $O(\epsilon)$ by

$$\epsilon\dot{y} = A_{22}y + B_2u, \quad y(t_0) = z_0 - A_{22}^{-1}A_{21}x_0 \tag{44}$$

Thus as $\epsilon \to 0$, the slow eigenvalues of Eq. (29) are approximated by $\lambda(A_0)$, and the fast eigenvalues are approximated by $\lambda(A_{22})/\epsilon$. It follows that if $\mathrm{Re}\{\lambda(A_0)\} < 0$ and $\mathrm{Re}\{\lambda(A_{22})\} < 0$, then there exists an $\epsilon^* > 0$ such that (29) is asymptotically stable for all $\epsilon \in (0, \epsilon^*]$. Furthermore, if the pair (A_0, B_0) and the pair (A_{22}, B_2) are each completely controllable (stabilizable), then there exists an $\epsilon^* > 0$ such that Eq. (29) is completely controllable (stabilizable) for all $\epsilon \in (0, \epsilon^*]$.

EXAMPLES

Example 1. An RLC Circuit

To complete our introductory example, we represent the *RLC* circuit in Eq. (1) using the state variables $x = v$ and $z = \dot{v}$:

$$\dot{x} = z \tag{45a}$$

$$\epsilon\dot{z} = -z - \frac{1}{RC}(x - u) \tag{45b}$$

where ϵ is the small time constant L/R. The unique solution of the quasi-steady-state equation (5) is $\bar{z} = -(\bar{x} - u)/(RC)$, which yields the reduced-order model

$$RC\dot{\bar{x}} = -\bar{x} + u \tag{46}$$

As expected, this is the RC equation (2). The boundary-layer system Eq. (9) for $y = z + (x - u)/(RC)$ is

$$\frac{dy}{d\tau} = -y, \quad y(t_0) = z(t_0) + \frac{1}{RC}(x(t_0) - u(t_0)) \tag{47}$$

Its solution $y = e^{-\tau}y(t_0) = -e^{-(R/L)t}y(t_0)$ approximates the fast transient neglected in the slow subsystem in Eq. (46). Tikhonov's Theorem is satisfied, because the fast subsystem in Eq. (47) is exponentially stable.

Example 2. A dc Motor

A common model for dc motors, shown in Fig. 4, under constant field excitation, consists of a mechanical torque equation and an equation for the electrical transient in the armature circuit, namely,

$$J\dot{\omega} = Ki - T_L \tag{48a}$$

$$L\dot{i} = -K\omega - Ri + u \tag{48b}$$

where i, u, R, and L are the armature current, voltage, resistance, and inductance, respectively, J is the combined moment of inertia of the motor and the load, ω is the angular speed, T_L is the load torque, and K is a motor design constant such that Ki and $K\omega$ are, respectively, the motor torque and the back emf (electromotive force).

We consider the case in which the electrical time constant $\tau_e = L/R$ is much smaller than the mechanical time constant $\tau_m = JR/K^2$ (3). Defining $\epsilon = \tau_e/\tau_m$, $x = \omega$, and $z = i$, we rewrite Eq. (48) as

$$\dot{x} = \frac{R}{\tau_m K}z - \frac{1}{J}T_L \tag{49a}$$

$$\epsilon\dot{z} = -\frac{K}{\tau_m R}x - \frac{1}{\tau_m}z + \frac{1}{\tau_m R}u \tag{49b}$$

Setting $\epsilon = 0$, we obtain from Eq. (49b)

$$0 = -K\bar{x} - R\bar{z} + u \tag{50}$$

Thus the quasi-steady state of z is

$$\bar{z} = \frac{u - K\bar{x}}{R} \tag{51}$$

which, when substituted in Eq. (49a), yields the slow mechanical subsystem

$$\tau_m\dot{\bar{x}} = -\bar{x} + \frac{1}{K}u - \frac{\tau_m}{J}T_L \tag{52}$$

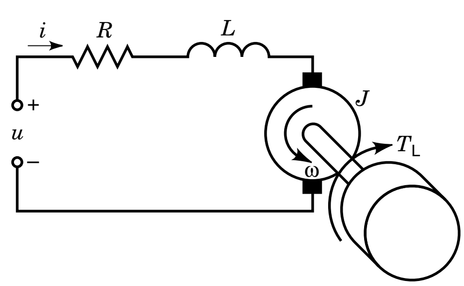

Figure 4. dc motor.

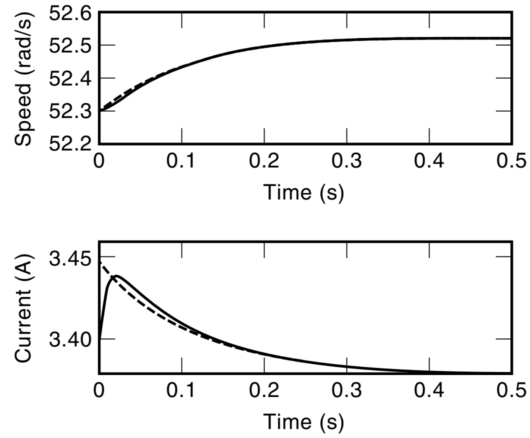

Figure 5. dc motor step response.

The parameters of a 1 hp (746 W) dc motor with a rated speed of 500 rpm (52.3 rad/s) are $R = 7.56\ \Omega$, $L = 0.055$ H, $K = 4.23$ Vs/rad, and $J = 0.136$ kg m^2. At the rated steady state condition, $T_L = 14.3$ N m, $i = 3.38$ A, and $u = 246.8$ V. The time constants are $\tau_e = 0.0073$ s and $\tau_m = 0.115$ s, resulting in $\epsilon = 0.063$. The response to a 1 V step increase in u of the full model in Eq. (48) (solid curves) and the slow subsystem in Eqs. (51) and (52) (dashed curves) is shown Fig. 5. Note that $\bar{x}$ is a good approximation of x. Initially there is a fast transient in z. After this "boundary layer" has decayed, $\bar{z}$ becomes a good approximation of z.

The fast electrical transient is approximated by the boundary-layer system

$$\tau_m\frac{dy}{d\tau} = -y, \quad y(0) = z(0) - \frac{u(0) - Kx(0)}{R} \tag{53}$$

which has the unique solution

$$y = e^{-\tau/\tau_m}y(0) = e^{-t/\tau_e}y(0) \tag{54}$$

Example 3. Multiple Slow Subsystems

To illustrate the possibility of several reduced-order models, we consider the singularly perturbed system

$$\dot{x} = x^2(1+t)/z \tag{55a}$$

$$\epsilon\dot{z} = -[z + (1+t)x]z[z - (1+t)] \tag{55b}$$

where the initial conditions are $x(0) = 1$ and $z(0) = z_0$. Setting $\epsilon = 0$ results in

$$0 = -[\bar{z} + (1+t)\bar{x}]\bar{z}[\bar{z} - (1+t)] \tag{56}$$

which has three distinct roots

$$\bar{z} = -(1+t)\bar{x}; \quad \bar{z} = 0; \quad \bar{z} = 1+t \tag{57}$$

Consider first the root $z = -(1+t)\bar{x}$. The boundary-layer system in Eq. (10) is

$$\frac{dy}{d\tau} = -y[y - (1+t)x][y - (1+t)x - (1+t)] \tag{58}$$

Taking $W(y) = y^2/2$, it can be verified that W satisfies the inequalities in Eqs. (15) and (16) for $y < (1 + t)\,x$. The reduced system

$$\dot{\bar{x}} = -\bar{x}, \quad \bar{x}(0) = 1 \tag{59}$$

has the unique solution $\bar{x}(t) = e^{-t}$ for all $t \geq 0$. The boundary-layer system with $t = 0$ and $x = 1$ is

$$\frac{d\hat{y}}{d\tau} = -\hat{y}(\hat{y}-1)(\hat{y}-2), \quad \hat{y}(0) = z_0 + 1 \tag{60}$$

and has a unique exponentially decaying solution $\hat{y}(\tau)$ for $z_0 + 1 \leq 1 - a$, that is, for $z_0 \leq -a < 0$ where $a > 0$ can be arbitrarily small.

Consider next the root $\bar{z} = 0$. The boundary-layer system in Eq. (10) is

$$\frac{dy}{d\tau} = -[y + (1+t)x]\,y\,[y - (1+t)] \tag{61}$$

By sketching the right-hand side function, it can be seen that the origin is unstable. Hence, Tikhonov's Theorem does not apply to this case and we rule out this root as a subsystem. Furthermore, $\dot{x}$ is not defined at $z = 0$.

Finally, the boundary-layer system for the root $\bar{z} = 1 + t$ is

$$\frac{dy}{d\tau} = -[y + (1+t) + (1+t)x][y + (1+t)]y \tag{62}$$

As in the first case, it can be shown that the origin is exponentially stable uniformly in (x, t). The reduced system

$$\dot{\bar{x}} = \bar{x}^2, \ \bar{x}(0) = 1 \tag{63}$$

has the unique solution $\bar{x}(t) = 1/(1 - t)$ for all $t \in [0, 1)$. Notice that $\bar{x}(t)$ has a finite escape time at $t = 1$. However, Tikhonov's Theorem still holds for $t \in [0, t_f]$ with $t_f < 1$. The boundary-layer system, with $t = 0$ and $x = 1$,

$$\frac{d\hat{y}}{d\tau} = -(\hat{y}+2)(\hat{y}+1)\hat{y}, \quad \hat{y}(0) = z_0 - 1 \tag{64}$$

has a unique exponentially decaying solution $\hat{y}(\tau)$ for $z_0 > a > 0$.

In summary, only two of the three roots in Eq. (57) give rise to valid reduced models. Tikhonov's Theorem applies to the root $\phi = -(1 + t)x$ if $z_0 < 0$ and to the root $\phi = 1 + t$ if $z_0 > 0$. Figure 6 shows z for four different values of z_0 of the full model (solid curves) and two for each reduced model (dashed curves).

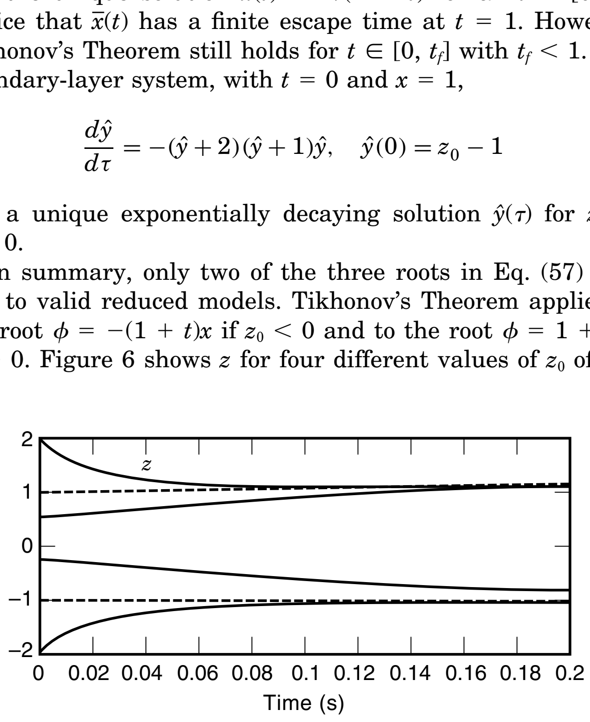

Figure 6. Response of system in Eq. (55) illustrating two slow subsystems.

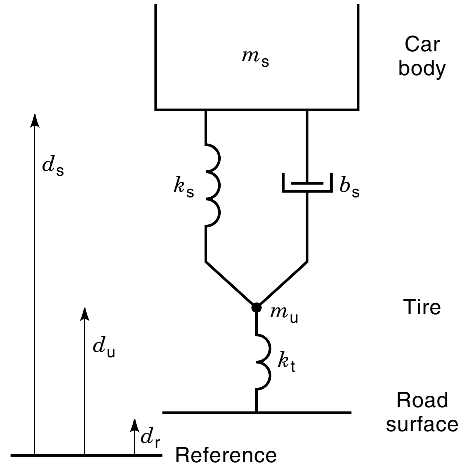

Figure 7. Quarter-car model.

Example 4. A Quarter-Car Model

A simplified quarter-car model is shown in Fig. 7, where m_s and m_u are the car body and tire masses, k_s and k_t are the spring constants of the strut and the tire, and b_s is the damper constant of the shock. The distances d_s, d_u, and d_r are the elevations of the car, the tire, and the road surface, respectively. From Newton's Law, the balance of forces acting on m_s and m_u results in the modeling equations

$$m_s\ddot{d}_s + b_s(\dot{d}_s - \dot{d}_u) + k_s(d_s - d_u) = 0 \tag{65a}$$

$$m_u\ddot{d}_u + b_s(\dot{d}_u - \dot{d}_s) + k_s(d_u - d_s) + k_t(d_u - d_r) = 0 \tag{65b}$$

In a typical car, the natural frequency $\sqrt{k_t/m_u}$ of the tire is much higher than the natural frequency $\sqrt{k_s/m_s}$ of the car body and the strut. We therefore define the parameter

$$\epsilon = \sqrt{\frac{k_s/m_s}{k_t/m_u}} = \sqrt{\frac{k_s m_u}{k_t m_s}} \tag{66}$$

The mass-spring system in Eq. (65) is of interest because it cannot be transformed into a standard model without an ϵ-dependent scaling. From Eq. (66), the tire stiffness $k_t = O(1/\epsilon^2)$ tends to infinity as $\epsilon \to 0$. For the tire potential energy $k_t(d_u - d_r)^2/2$ to remain bounded, the displacement $d_u - d_r$ must be $O(\epsilon)$, that is, the scaled displacement $(d_u - d_r)/\epsilon$ must remain finite. Thus to express Eq. (65) in the standard singularly perturbed form, we introduce the slow and fast variables as

$$x = \begin{bmatrix} d_s - d_u \\ \dot{d}_s \end{bmatrix}, \quad z = \begin{bmatrix} (d_u - d_r)/\epsilon \\ \dot{d}_u \end{bmatrix} \tag{67}$$

and $u = \dot{d}_r$ as the disturbance input. The resulting model is

$$\dot{x} = A_{11}x + A_{12}z + B_1u \tag{68a}$$

$$\epsilon\dot{z} = A_{21}x + A_{22}z + B_2u \tag{68b}$$

where

$$A_{11} = \begin{bmatrix} 0 & 1 \\ -k_s/m_s & -b_s/m_s \end{bmatrix}, \quad A_{12} = \begin{bmatrix} 0 & -1 \\ 0 & b_s/m_s \end{bmatrix}, \quad B_1 = \begin{bmatrix} 0 \\ 0 \end{bmatrix}$$
$$A_{21} = \begin{bmatrix} 0 & 0 \\ \alpha k_s/m_s & \alpha b_s/m_s \end{bmatrix}, \quad A_{22} = \begin{bmatrix} 0 & 1 \\ -k_s/m_s & -\alpha b_s/m_s \end{bmatrix},$$
$$B_2 = \begin{bmatrix} -1 \\ 0 \end{bmatrix} \tag{69}$$

and

$$\alpha = \sqrt{\frac{k_s m_s}{k_t m_u}} \tag{70}$$

The parameters of a typical passenger car are m_s = 504.5 kg, m_u = 62 kg, b_s = 1,328 Ns/m, k_s = 13,100 N/m, k_t = 252,000 N/m, and α = 0.65. In this case, ϵ = 0.08 and the time scales of the body (slow) and the tire (fast) are well separated.

To illustrate the approximation provided by the two-time-scale analysis, the slow and fast eigenvalues of the uncorrected subsystems in Eqs. (43) and (44) are found to be $-2.632 \pm j6.709$ and $-10.710 \pm j62.848$, respectively, which are within 4% of the eigenvalues $-2.734 \pm j7.018$ and $-9.292 \pm j60.287$ of the full-order model. If a higher accuracy is desired, the series expansion in Eq. (34) can be used to add the first-order correction terms to the diagonal blocks of Eq. (39), resulting in the approximate slow eigenvalues $-2.705 \pm j6.982$ and fast eigenvalues $-9.394 \pm j60.434$, and thus reducing the errors to less than 0.5%.

Example 5. A High-Gain Power Rectifier

Many modern control systems include power electronic rectifiers as actuators. An example is a static excitation system that controls the field voltage E_{fd} of a synchronous machine shown in Fig. 8 (4). The synchronous machine is modeled as

$$\dot{x} = f(x, E_{fd}) \tag{71a}$$
$$V_T = h(x) \tag{71b}$$

where x is the machine state vector including the flux variables and the scalar output V_T is the generator terminal voltage. Here we focus on the exciter system which, from Fig. 8, is described by

$$T_M \dot{E} = -E - K_M K_G E_{fd} + K_M V_R \tag{72a}$$
$$E_{fd} = V_B(x) E \tag{72b}$$

where T_M is a time constant and K_M and K_G are gains.

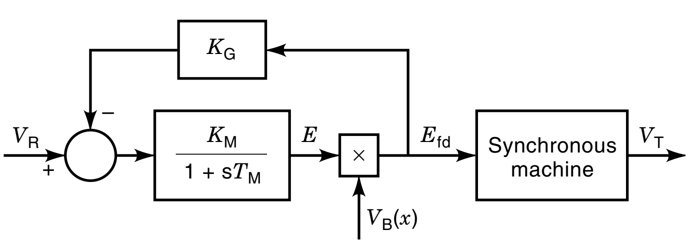

Figure 8. Static excitation system.

Following the input signal V_R, the voltage E modulates the supply voltage $V_B(x)$ to control E_{fd}. The supply voltage $V_B(x)$ is a function of x and is typically within the range of 4–8 per unit on the base field voltage.

Under normal operating conditions, the product of the rectifier gain and the supply voltage $K_M V_B(x)$ is very high. This motivates us to define ϵ as

$$\epsilon = \frac{1}{K_M \overline{V}_B} \ll 1 \tag{73}$$

where $\overline{V}_B$ is a constant of the order of magnitude of $V_B(x)$, that is, the ratio $\beta(x) = V_B(x)/\overline{V}_B = O(1)$. Using E_{fd} as the state variable instead of E, Eq. (72) is rewritten as

$$T_M \dot{E}_{fd} = -\left[1 + K_G K_M V_B(x) - \frac{T_M}{V_B(x)} \gamma(x, E_{fd})\right] E_{fd} + K_M V_B(x) V_R \tag{74}$$

where $\gamma(x, E_{fd}) = [\partial V_B(x)/\partial x]\dot{x}$ is bounded. Using ϵ, Eq. (74) becomes

$$\epsilon \dot{E}_{fd} = -\left[\frac{K_G \beta(x) + \epsilon}{T_M} - \frac{\epsilon}{V_B(x)} \gamma(x, E_{fd})\right] E_{fd} + \frac{\beta(x)}{T_M} V_R \tag{75}$$

which yields, as $\epsilon \to 0$, the quasi-steady state

$$\overline{E}_{fd} = \frac{1}{K_G} V_R \tag{76}$$

In a typical rectifier system, K_G = 1, K_M = 7.93, and T_M = 0.4 s. For $\overline{V}_B$ = 6, we obtain ϵ = 0.021. The time-scales are well separated, which allows us to achieve high accuracy with singular perturbation approximations.

Example 6. Slow Manifold in a Synchronous Machine

We now proceed to illustrate the use of the slow manifold concept as a modeling tool. In most cases, the solution of the manifold condition in Eq. (20) is evaluated approximately as a power series in ϵ. However, for a synchronous machine model, the slow manifold, which excludes stator circuit transients, can be calculated exactly, as shown by Kokotovic and Sauer (5).

The synchronous machine model with one damper winding in the quadrature axis is

$$\frac{d\delta}{dt} = \omega - \omega_s \tag{77a}$$
$$\frac{2H}{\omega_s}\frac{d\omega}{dt} = T_m + \left(\frac{1}{L'_q} - \frac{1}{L'_d}\right)\psi_d\psi_q + \frac{1}{L'_q}\psi_d E'_d + \frac{1}{L'_d}\psi_q E'_q \tag{77b}$$
$$T'_{do}\frac{dE'_q}{dt} = -\frac{L_d}{L'_d}E'_q - \frac{L_d - L'_d}{L'_d}\psi_d + E_{fd} \tag{77c}$$
$$T'_{qo}\frac{dE'_d}{dt} = -\frac{L_q}{L'_q}E'_d - \frac{L_q - L'_q}{L'_q}\psi_q \tag{77d}$$
$$\frac{1}{\omega_s}\frac{d\psi_d}{dt} = -\frac{R_a}{L'_d}\psi_d + \frac{R_a}{L'_d}E'_q + \frac{\omega}{\omega_s}\psi_q + V\sin\delta \tag{77e}$$
$$\frac{1}{\omega_s}\frac{d\psi_q}{dt} = -\frac{R_a}{L'_q}\psi_q - \frac{R_a}{L'_q}E'_d - \frac{\omega}{\omega_s}\psi_d + V\cos\delta \tag{77f}$$

where δ, ω, and H are the generator rotor angle, speed, and inertia, respectively, (E'_d, E'_q), (ψ_d, ψ_q), (T'_{do}, T'_{qo}), (L_d, L_q), and

(L_d', L_q') are the d- and q-axis voltages, flux linkages, open-circuit time constants, synchronous reactances, and transient reactances, respectively, R_a is the stator resistance, T_m is the input mechanical torque, E_{fd} is the excitation voltage, and ω_s is the system frequency.

In the model shown in Eq. (77), the slow variables are δ, ω, E_d', and E_q', and the fast variables are ψ_d and ψ_q. The singular perturbation parameter can be defined as $\epsilon = 1/\omega_s$.

If the stator resistance is neglected, that is, $R_a = 0$, it can be readily verified that the slow manifold condition in Eq. (20) gives the exact slow invariant manifold

$$\psi_d = V\cos\delta, \quad \psi_q = -V\sin\delta \tag{78}$$

These expressions can be substituted into Eqs. (77a)–(77d) to obtain a fourth-order slow subsystem.

If the initial condition [$\psi_d(0)$, $\psi_q(0)$] is not on the manifold shown in Eq. (78), then using the fast variables

$$y_d = \psi_d - V\cos\delta, \quad y_q = \psi_q + V\sin\delta \tag{79}$$

we obtain the fast subsystem

$$\epsilon\frac{dy_d}{dt} = \frac{\omega}{\omega_s}y_q, \qquad y_d(0) = \psi_d(0) - V\cos\delta(0) \tag{80a}$$

$$\epsilon\frac{dy_q}{dt} = -\frac{\omega}{\omega_s}y_d, \quad y_q(0) = \psi_q(0) + V\sin\delta(0) \tag{80b}$$

where the state ω appears as a time-varying coefficient.

When the stator resistance R_a is nonzero, the slow manifold condition can no longer be solved exactly. Instead, the leading terms in the power series expansion in Eq. (21) can be computed to obtain any desired approximation of the slow manifold.

Example 7. Van der Pol Oscillator

A classical use of the slow manifold concept is to demonstrate the relaxation oscillation phenomenon in a Van der Pol oscillator, modeled in the state-space form as (6)

$$\dot{x} = z \tag{81a}$$

$$\epsilon\dot{z} = -x + z - \tfrac{1}{3}z^3 \tag{81b}$$

For ϵ small, the slow manifold is approximated by

$$g(x,z) = -x + z - \tfrac{1}{3}z^3 = 0 \tag{82}$$

which is shown as the curve $ABCD$ in Fig. 9. For the roots $z = \phi(x)$ on the branches AB and CD

$$\frac{\partial g}{\partial z} = 1 - z^2 < 0 \tag{83}$$

and the eigenvalue condition of Tikhonov's Theorem is satisfied because $z^2 > 1$. Therefore, the branches AB and CD are attractive, that is, trajectories converging to these two branches will remain on them, moving toward either the point B or C. However, the root on the branch BC is unstable because $z^2 < 1$; hence, this branch of the slow manifold is repulsive.

Figure 9 shows vertical trajectories converging toward AB and CD, because $\epsilon \neq 0$. The mechanism of two interior (rather than boundary) layers, from B to D' and from C to A' is clear from this phase portrait. The relaxation oscillation forming the limit cycle A'-B-D'-C consists of the slow motions from A' to B and D' to C, connected with fast jumps (layers) from B to D' and from C to A'. When ϵ is increased to a small positive value, this limit cycle is somewhat deformed, but its main character is preserved. This observation is one of the cornerstones of the classical nonlinear oscillation theory (7), which has many applications in engineering and biology.

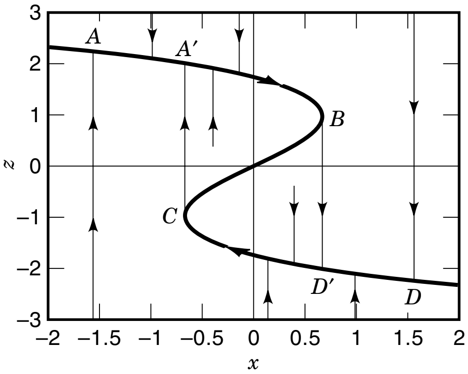

Figure 9. Phase portrait of the Van der Pol oscillator.

STABILITY ANALYSIS

We consider the autonomous singularly perturbed system in Eq. (17). Let the origin ($x = 0$, $z = 0$) be an isolated equilibrium point and the functions f and g be locally Lipschitz in a domain that contains the origin. We want to analyze stability of the origin by examining the reduced and boundary-layer models. Let $z = \phi(x)$ be an isolated root of $0 = g(x,z)$ defined in a domain $D_1 \in R^n$ that contains $x = 0$, such that $\phi(x)$ is continuous and $\phi(0) = 0$. With the change of variables $y = z - \phi(x)$, the singularly perturbed system is represented in the new coordinates as

$$\dot{x} = f(x, y + \phi(x)) \tag{84a}$$

$$\epsilon\dot{y} = g(x, y + \phi(x)) - \epsilon\frac{\partial\phi}{\partial x}f(x, y + \phi(x)) \tag{84b}$$

The reduced system $\dot{x} = f(x, \phi(x))$ has equilibrium at $x = 0$, and the boundary-layer system $dy/d\tau = g(x,y + \phi(x))$ has equilibrium at $y = 0$. The main theme of the two-time-scale stability analysis is to assume that, for each of the two systems, the origin is asymptotically stable and that we have a Lyapunov function that satisfies the conditions of Lyapunov's Theorem. In the case of the boundary-layer system, we require asymptotic stability of the origin to hold uniformly in the frozen parameter x. Viewing the full singularly perturbed system (84) as an interconnection of the reduced and boundary-layer systems, we form a composite Lyapunov function candidate for the full system as a linear combination of the Lyapunov functions for the reduced and boundary-layer systems. We then proceed to calculate the derivative of the composite Lyapunov function along the trajectories of the full system and verify, under reasonable growth conditions on f and g, that it is negative definite for sufficiently small ϵ.

Let $V(x)$ be a Lyapunov function for the reduced system such that

$$\frac{\partial V}{\partial x} f(x, \phi(x)) \le -\alpha_1 \psi_1^2(x), \quad \forall\, x \in D_1 \tag{85}$$

where $\psi_1(x)$ is a positive definite function. Let $W(x, y)$ be a Lyapunov function for the boundary-layer system such that

$$\frac{\partial W}{\partial y} g(x, y + \phi(x)) \le -\alpha_2 \psi_2^2(y), \quad \forall (x, y) \in D_1 \times D_2 \tag{86}$$

where $D_2 \subset R^m$ is a domain that contains $y = 0$, and $\psi_2(y)$ is a positive definite function. We allow the Lyapunov function W to depend on x because x is a parameter of the system and Lyapunov functions may, in general, depend on the system's parameters. Because x is not a true constant parameter, we must keep track of the effect of the dependence of W on x. To ensure that the origin of the boundary-layer system is asymptotically stable uniformly in x, we assume that $W(x, y)$ satisfies

$$W_1(y) \le W(x, y) \le W_2(y), \quad \forall (x, y) \in D_1 \times D_2 \tag{87}$$

for some positive definite continuous functions W_1 and W_2. Now consider the composite Lyapunov function candidate

$$\nu(x, y) = (1 - d)V(x) + dW(x, y), \quad 0 < d < 1 \tag{88}$$

where the constant d is to be chosen. Calculating the derivative of ν along the trajectories of the full system in Eq. (84), we obtain

$$\begin{aligned}\dot{\nu} &= (1-d)\frac{\partial V}{\partial x} f(x, \phi(x)) + \frac{d}{\epsilon}\frac{\partial W}{\partial y} g(x, y + \phi(x)) \\ &\quad + (1-d)\frac{\partial V}{\partial x}[f(x, y + \phi(x)) - f(x, \phi(x))] \\ &\quad + d\left(\frac{\partial W}{\partial x} - \frac{\partial W}{\partial y}\frac{\partial \phi}{\partial x}\right) f(x, y + \phi(x))\end{aligned} \tag{89}$$

We have represented the derivative $\dot{\nu}$ as the sum of four terms. The first two terms are the derivatives of V and W along the trajectories of the reduced and boundary-layer systems. These two terms are negative definite in x and y, respectively, by the inequalities in Eqs. (85) and (86). The other two terms represent the effect of the interconnection between the slow and fast dynamics, which is neglected at $\epsilon = 0$. Suppose these terms satisfy the interconnection conditions

$$\frac{\partial V}{\partial x}[f(x, y + \phi(x)) - f(x, \phi(x))] \le \beta_1 \psi_1(x)\psi_2(y) \tag{90}$$

$$\left(\frac{\partial W}{\partial x} - \frac{\partial W}{\partial y}\frac{\partial \phi}{\partial x}\right) f(x, y + \phi(x)) \le \beta_2 \psi_1(x)\psi_2(y) + \gamma \psi_2^2(y) \tag{91}$$

for some nonnegative constants β_1, β_2, and γ. Using the inequalities in Eqs. (85), (86), (90), and (91), we obtain

$$\dot{\nu} \le -\begin{bmatrix}\psi_1(x) \\ \psi_2(y)\end{bmatrix}^T \begin{bmatrix}(1-d)\alpha_1 & -\frac{1}{2}(1-d)\beta_1 - \frac{1}{2}d\beta_2 \\ -\frac{1}{2}(1-d)\beta_1 - \frac{1}{2}d\beta_2 & d\left(\frac{\alpha_2}{\epsilon} - \gamma\right)\end{bmatrix} \begin{bmatrix}\psi_1(x) \\ \psi_2(y)\end{bmatrix} \tag{92}$$

The right-hand side of the last inequality is a quadratic form in $(\psi_1(x), (\psi_2(y))$. The quadratic form is negative definite when

$$d(1-d)\alpha_1\left(\frac{\alpha_2}{\epsilon} - \gamma\right) > \tfrac{1}{4}[(1-d)\beta_1 + d\beta_2]^2 \tag{93}$$

For any d, there is an ϵ_d such that Eq. (93) is satisfied for $\epsilon < \epsilon_d$. The maximum value of ϵ_d occurs at $d^* = \beta_1/(\beta_1 + \beta_2)$ and is given by

$$\epsilon^* = \frac{\alpha_1\alpha_2}{\alpha_1\gamma + \beta_1\beta_2} \tag{94}$$

It follows that the origin is asymptotically stable for all $\epsilon < \epsilon^*$. Note that the functions $\psi_1(x)$ and $\psi_2(x)$ and the interconnection conditions in Eqs. (90) and (91) should be carefully constructed so that ϵ^* may not be unnecessarily conservative.

As an illustration of the preceding Lyapunov analysis, consider the second-order system

$$\dot{x} = f(x, z) = x - x^3 + z \tag{95a}$$

$$\epsilon\dot{z} = g(x, z) = -x - z \tag{95b}$$

which has a unique equilibrium point at the origin. Let $y = z - \phi(x) = z + x$. For the reduced system $\dot{x} = -x^3$, we take $V(x) = \frac{1}{4}x^4$, which satisfies Eq. (85) with $\psi_1(x) = |x|^3$ and $\alpha_1 = 1$. For the boundary-layer system $dy/d\tau = -y$, we take $W(y) = \frac{1}{2}y^2$, which satisfies Eq. (86) with $\psi_2(y) = |y|$ and $\alpha_2 = 1$. As for the interconnection conditions in Eqs. (90) and (91), we have

$$\frac{\partial V}{\partial x}[f(x, y + \phi(x)) - f(x, \phi(x))] = x^3 y \le \psi_1\psi_2 \tag{96}$$

$$\frac{\partial W}{\partial y} f(x, y + \phi(x)) = y(-x^3 + y) \le \psi_1\psi_2 + \psi_2^2 \tag{97}$$

Note that $\partial W/\partial x = 0$. Hence, Eqs. (90) and (91) are satisfied with $\beta_1 = \beta_2 = \gamma = 1$. Therefore, the origin is asymptotically stable for $\epsilon < \epsilon^* = 0.5$. Because all the conditions are satisfied globally and $\nu(x, y) = (1 - d)V(x) + dW(y)$ is radially unbounded, the origin is globally asymptotically stable for $\epsilon < 0.5$.

The preceding two-time-scale stability analysis can be extended to the nonautonomous singularly perturbed system in Eq. (3). For sufficiently smooth f, g, and ϕ, it can be shown that if the origin of the reduced system is exponentially stable, and the origin of the boundary-layer system is exponentially stable, uniformly in (t, x), then the origin of the full system in Eq. (3) is exponentially stable for sufficiently small ϵ. The same conditions ensure the validity of Tikhonov's Theorem for all $t \ge t_0$. Note that the earlier statement of Tikhonov's Theorem, which does not require exponential stability of the reduced system, is valid only on a compact time interval $[t_0, t_f]$ for a given t_f.

COMPOSITE FEEDBACK CONTROL

The impetus for the systematic decomposition of the slow and fast subsystems in singularly perturbed systems can be readily extended to the separate control design of the slow and fast dynamics. As will be shown, the crucial idea is to compensate for the quasi-steady state in the fast variable.

Consider the nonlinear singularly perturbed system

$$\dot{x} = f(x, z, u) \tag{98a}$$
$$\epsilon\dot{z} = g(x, z, u) \tag{98b}$$

and suppose the equation $0 = g(x, z, u)$ has a unique root $z = \phi(x, u)$ in a domain D that contains the origin. A separated slow and fast design is succinctly captured in the composite control

$$u = u_s + u_f \tag{99}$$

where u_s is a slow control function of x

$$u_s = \Gamma_s(x) \tag{100}$$

and u_f is a fast control function of both x and z

$$u_f = \Gamma_f(x, z) \tag{101}$$

Applying the control in Eq. (99) to the full model in Eq. (98), we obtain

$$\dot{x} = f(x, z, \Gamma_s(x) + \Gamma_f(x, z)) \tag{102a}$$
$$\epsilon\dot{z} = g(x, z, \Gamma_s(x) + \Gamma_f(x, z)) \tag{102b}$$

The fast control $\Gamma_f(x, z)$ must guarantee that $z = \phi(x, \Gamma_s(x))$ is a unique solution to the equation

$$0 = g(x, z, \Gamma_s(x) + \Gamma_f(x, z)) \tag{103}$$

in the domain D. Furthermore, we require the fast control to be inactive on the manifold in Eq. (103), that is,

$$\Gamma_f(x, \phi(x, \Gamma_s(x))) = 0 \tag{104}$$

Then the slow and fast subsystems become, respectively,

$$\dot{x} = f(x, \phi(x, \Gamma_s(x)), \Gamma_s(x)) \tag{105}$$
$$\epsilon\dot{z} = g(x, z, \Gamma_s(x) + \Gamma_f(x, z)) \tag{106}$$

To obtain controllers so that the equilibrium ($x = 0, z = 0$) is asymptotically stable, $\Gamma_s(x)$ must be designed so that a Lyapunov function $V(x)$ satisfying Eq. (85) can be found for the slow subsystem in Eq. (105), and $\Gamma_f(x, z)$ must be designed so that a Lyapunov function $W(x, z)$ satisfying Eq. (86) can be found for the fast subsystem in Eq. (106). Furthermore, the interconnection conditions corresponding to Eqs. (90) and (91) must be satisfied, so that a composite Lyapunov function similar to Eq. (88) can be used to establish the asymptotic stability of the equilibrium.

Specializing the composite control design to the linear singularly perturbed system in Eq. (29), we design the slow and fast controls as

$$\Gamma_s = G_0 x = G_0\xi + O(\epsilon) \tag{107}$$
$$\Gamma_f = G_2[z + A_{22}^{-1}(A_{21}x + B_{22}G_0 x)] \triangleq G_2 y \tag{108}$$

such that the closed-loop subsystems in Eqs. (43) and (44) to $O(\epsilon)$

$$\dot{\xi} = (A_0 + B_0 G_0)\xi \tag{109}$$
$$\epsilon\dot{y} = (A_{22} + B_2 G_2)y \tag{110}$$

have the desired properties. Thus the composite control in Eq. (99) is

$$u = G_0 x + G_2[z + A_{22}^{-1}(A_{21} + B_2 G_0)x] = G_1 x + G_2 z \tag{111}$$

where

$$G_1 = (I_m + G_2 A_{22}^{-1} B_2)G_0 + G_2 A_{22}^{-1} A_{21} \tag{112}$$

When Eq. (111) is applied to the full-order model in Eq. (29), the slow and fast dynamics of the closed-loop system are approximated to $O(\epsilon)$ by the slow and fast subsystems in Eqs. (109) and (110), respectively.

If the pairs (A_0, B_0) and (A_{22}, B_2) are completely controllable, the results here point readily to a two-time-scale pole-placement design in which G_0 and G_2 are designed separately to place the slow eigenvalues of $A_0 + B_0G_0$ and the fast eigenvalues of $(A_{22} + B_2G_2)/\epsilon$ at the desired locations. Then the eigenvalues of the closed-loop full-order system will approach these eigenvalues as ϵ tends to zero.

The composite feedback control is also fundamental in near-optimal control design of linear quadratic regulators for two-time-scale systems. Consider the optimal control of the linear singularly perturbed system in Eq. (29) to minimize the performance index

$$J(u) = \frac{1}{2}\int_0^\infty (q^T q + u^T R u)\, dt, \quad R > 0 \tag{113}$$

where

$$q(t) = C_1 x(t) + C_2 z(t) \tag{114}$$

Following the slow and fast subsystem decomposition in Eqs. (43) and (44), we separate $q(t)$ into its slow and fast components as

$$q(t) = q_s(t) + q_f(t) + O(\epsilon)) \tag{115}$$

where

$$q_s(t) = C_0\xi + D_0 u_s \tag{116}$$

with

$$C_0 = C_1 + C_2 A_{22}^{-1} A_{21}, \quad D_0 = -C_2 A_{22}^{-1} B_2 \tag{117}$$

and

$$q_f(t) = C_2 y \tag{118}$$

From the subsystems in Eqs. (43) and (44) and the decomposition in Eq. (115), the linear quadratic regulator problem in Eq. (113) can be solved from two lower-order subproblems.

Slow Regulator Problem

Find the slow control u_s for the slow subsystem in Eqs. (43) and (116) to minimize

$$\begin{aligned} J_s(u_s) &= \frac{1}{2}\int_0^\infty (q_s^T q_s + u_s^T R u_s)\, dt, \quad R > 0 \\ &= \frac{1}{2}\int_0^\infty (\xi^T C_0^T C_0 \xi + 2u_s^T D_0^T C_0^T \xi + u_s^T R_0 u_s)\, dt \end{aligned} \tag{119}$$

where

$$R_0 = R + D_0^T D_0 \tag{120}$$

If the triple (C_0, A_0, B_0) is stabilizable and detectable (observable), then there exists a unique positive-semidefinite (positive-definite) stabilizing solution K_s of the matrix Riccati equation

$$\begin{aligned} 0 = & -K_s(A_0 - B_0R_0^{-1}D_0^TC_0) - (A_0 - B_0R_0^{-1}D_0^TC_0)^TK_s \\ & + K_sB_0R_0^{-1}B_0K_s - C_0^T(I - D_0R_0^{-1}N_0^T)C_0 \end{aligned} \tag{121}$$

and the optimal control is

$$u_s = -R_0^{-1}(D_0^TC_0 + B_0^TK_s)\xi = G_0\xi \tag{122}$$

Fast Regulator Problem

Find the fast control u_f for the fast subsystem in Eqs. (44) and (118) to minimize

$$\begin{aligned} J_f(u_f) &= \frac{1}{2}\int_0^\infty (q_f^Tq_f + u_f^TRu_f)\,dt, \quad R > 0 \\ &= \frac{1}{2}\int_0^\infty (y^TC_2^TC_2y + u_f^TRu_f)\,dt \end{aligned} \tag{123}$$

If the triple (C_2, A_{22}, B_2) is stabilizable and detectable (observable), then there exists a unique positive-semidefinite (positive-definite) stabilizing solution K_f of the matrix Riccati equation

$$0 = -K_fA_{22} - A_{22}^TK_f + K_fB_2R^{-1}B_2K_f - C_2^TC_2 \tag{124}$$

and the optimal control is

$$u_f = -R^{-1}B_2^TK_fy = G_{22}y \tag{125}$$

The following results are from Reference (8).

Theorem 1.

1. If the triples (C_0, A_0, B_0) and (C_2, A_{22}, B_2) are stabilizable and detectable (observable), then there exists an $\epsilon^* > 0$ such that for all $\epsilon \in (0, \epsilon^*]$, an optimal control exists for the linear regulator problem (113) with an optimal performance J_{opt}.
2. The composite control in Eq. (111)

$$\begin{aligned} u_c = & -[(I - R^{-1}B_2^TK_fA_{22}^{-1}B_2)R_0^{-1}(D_0^TC_0 + B_0^TK_s) \\ & + R^{-1}B_2^TK_fA_{22}^{-1}A_{21}]x - R^{-1}B_2^TK_fz \end{aligned} \tag{126}$$

applied to the system in Eq. (29) achieves an $O(\epsilon^2)$ approximation of J_{opt}, that is,

$$J(u_c) = J_{opt} + O(\epsilon^2) \tag{127}$$

3. If A_{22} is stable, then the slow control in Eq. (122)

$$u_s = -R_0^{-1}(D_0^TC_0 + B_0^TK_s)x \tag{128}$$

applied to the system in Eq. (29) achieves an $O(\epsilon)$ approximation of J_{opt}, that is,

$$J(u_s) = J_{opt} + O(\epsilon) \tag{129}$$

In Theorem 1.1, an asymptotic expansion exists for the solution to the matrix Riccati equation associated with the full linear regulator problem. Theorem 1.3 is one of the robustness results with respect to fast unmodeled dynamics, that is, if the fast dynamics is asymptotically stable, a feedback control containing only the slow dynamics would not destabilize the fast dynamics.

APPLICATIONS TO LARGE POWER SYSTEMS

In this section, we analyze a large power system as an example of time-scales arising in an interconnected systems. A power system dispersed over a large geographical area tends to have dense meshes of power networks serving heavily populated areas and many fewer transmission lines interconnecting these urban centers. When such a system is subject to a disturbance, it is observed that groups of closely located machines would swing coherently at a frequency that is lower than the frequency of oscillation within the coherent groups. Singular perturbation techniques have been successfully applied to these large power networks to reveal this two-time-scale behavior (9).

Consider the linearized electromechanical model of an n-machine power system in the second-order form with damping neglected

$$M\ddot{\delta} = K\delta \tag{130}$$

where $\delta \in R^n$ is the machine rotor angle vector, M is the diagonal matrix of machine inertias, and K is the stiffness matrix determined by the network impedances. Assume that the system in Eq. (130) has r tightly connected areas, with the connections between the areas being relatively fewer. In this case, we decompose K into

$$K = K^I + \epsilon K^E \tag{131}$$

where K^I is the stiffness matrix due to the impedances internal to the areas, and K^E is the stiffness matrix due to the impedances external to the areas and scaled by the small parameter ϵ that represents the ratio of the external to the internal connection strength.

For illustrative purposes, we let $r = 2$, with r_1 machines in area 1 and r_2 machines in area 2. Arranging the machines in area 1 to appear first in δ, K^I has a block-diagonal structure

$$K^I = \text{block-diag}(K_1^I, K_2^I) \tag{132}$$

A particular property of the $r_i \times r_i$ matrix K_i^I, $i = 1, 2$, is that each of the rows in K_i^I will sum to zero. If $\epsilon = 0$, this conservation property results in a slow mode in each area. When $\epsilon \neq 0$, the slow mode from each area will interact to form the low-frequency interarea oscillatory mode.

To reveal this slow dynamics, we define a grouping matrix

$$U = \begin{bmatrix} \mathbf{1}_{r_1} & 0 \\ 0 & \mathbf{1}_{r_2} \end{bmatrix} \tag{133}$$

where $\mathbf{1}_{r_i}$ is an $r_i \times 1$ column vector of all ones. Using U, we introduce the aggregate machine angles weighted according to the inertia as the slow variables

$$\delta_a = (U^TMU)^{-1}U^TM\delta = C\delta \tag{134}$$

and the difference angles with respect to the first machine in each area as the fast variables

$$\delta_d = G\delta \tag{135}$$

where

$$G = \begin{bmatrix} -\mathbf{1}_{r_1-1} & I_{r_1-1} & 0 & 0 \\ 0 & 0 & -\mathbf{1}_{r_2-1} & I_{r_2-1} \end{bmatrix} \tag{136}$$

Noting that $CM^{-1}K^I = 0$ and $K^IU = 0$, that is, C is in the left null space of $M^{-1}K^I$ and U is in the right null space of K^I, the system in Eq. (130) in the new variables become

$$\ddot{\delta}_a = \epsilon CM^{-1}K^EU\delta_a + \epsilon CM^{-1}K^EG^+\delta_d \tag{137a}$$

$$\ddot{\delta}_d = \epsilon GM^{-1}K^EU\delta_a + (GM^{-1}K^IG^+ + \epsilon GM^{-1}K^EG^+)\delta_d \tag{137b}$$

where $G^+ = G^T(GG^T)^{-1}$. The system in Eq. (137) clearly points to the two-time-scale behavior in which the right-hand side of Eq. (137a) is $O(\epsilon)$, indicating that δ_a is a slow variable. The method can readily be extended to systems with $r > 2$ areas.

Based on this time-scale interpretation, a grouping algorithm using the slow eigensubspace has been proposed to find the tightly connected machines if they are not known ahead of time. Then the areas whose internal dynamics are of less interest can be aggregated into single machine equivalents to capture only the slow dynamics. This concept, together with some more recently developed algorithms, has been implemented in computer software to reduce large power systems to smaller models suitable for stability analysis and control design (10).

FURTHER READING

Singular perturbation techniques have been successfully applied to the analysis and design of many control systems other than those discussed in this article. For our concluding remarks, we briefly comment on some of these applications as extensions of the results already discussed.

The two-time-scale properties can also be used to characterize transfer functions of singularly perturbed systems (11). In a linear discrete-time two-time-scale system, the slow dynamics arise from the system eigenvalues close to the unit circle, whereas the fast dynamics are a result of those eigenvalues close to the origin. The two-time-scale analysis for continuous-time systems can be readily extended to discrete-time singularly perturbed systems (12).

An application of the stability results is to determine the robustness of a control design. For example, Khalil (13) shows a simple example where a static output feedback designed without considering the parasitic effects would lead to an instability in the fast dynamics. Another result shows that in adaptive control, the rate of adaptation must be sufficiently slow so that the unmodeled fast dynamics would not cause destabilization (14).

The composite control has also been applied to solve optimal regulator problems for nonlinear singularly perturbed systems (15). Recently, composite control results for H_∞ optimal control of singularly perturbed systems have been obtained (16, 17). The composite control idea can also be used to establish the time scales in a closed-loop system induced by a high-gain control (18).

Singular perturbation methods also have significant applications in flight control problems (19, 20). For example, two-point boundary-value problems arising from trajectory optimization can be solved by treating the fast maneuvers and the slower cruise dynamics separately.

The slow coherency and aggregation technique is also applicable to other large-scale systems, such as Markov chains (21) and multi-market economic systems (22). These systems belong to the class of singularly perturbed systems in the nonstandard form, of which an extended treatment can be found in Ref. 23.

A topic not covered here is the filtering and stochastic control of singularly perturbed systems with input noise. As $\epsilon \to 0$, the fast dynamics will tend to a white noise. Although the problem can be studied in two-time-scales, the convergence of the optimal solution requires that the noise input in the fast dynamics be either colored or asymptotically small (24).

Another topic not covered is the control of distributed parameter systems possessing two-time-scale properties. Averaging and homogenization techniques are also a class of two-time-scale methods (25). More developments are expected in this area.

In more complex singularly perturbed systems, jump behaviors may arise not only at the end points but also in interior layers. Reference 27, beside being an introductory text to singular perturbations, contains a detailed treatment of such phenomena. It also contains a historical development of singular perturbations.

The singular perturbation results presented in this article represent developments over a period of three decades and contribute to the advances of modern control theory. As new control problems are proposed and new applications are discovered for systems with time-scales, we expect that singular perturbation methods will also be extended accordingly to provide simpler models to gain useful design insights into these new problems.

BIBLIOGRAPHY

1. P. K. Kokotovic, H. K. Khalil, and J. O'Reilly, *Singular Perturbation Methods in Control: Analysis and Design,* London: Academic Press, 1986.
2. P. K. Kokotovic and H. K. Khalil (eds.), *Singular Perturbations in Systems and Control,* New York: IEEE Press, 1986.
3. A. E. Fitzgerald, C. Kingsley, and A. Kusko, *Electric Machinery,* 3rd ed., New York: McGraw-Hill, 1973.
4. IEEE Committee Report, Excitation system models for power system stability studies, *IEEE Trans. Power Appar. Syst.,* **PAS-100**: 494–509, 1981.
5. P. V. Kokotovic and P. W. Sauer, Integral manifold as a tool for reduced-order modeling of nonlinear systems: A synchronous machine case study, *IEEE Trans. Circuits Syst.,* **36**: 403–410, 1985.
6. H. K. Khalil, *Nonlinear Systems,* 2nd ed., Upper Saddle River, NJ: Prentice-Hall, 1996.

7. J. K. Hale, *Ordinary Differential Equations,* Huntington, NY: Krieger Publisher Co., 1980.
8. J. H. Chow and P. V. Kokotovic, A decomposition of near-optimum regulators for systems with slow and fast modes, *IEEE Trans. Autom. Control,* **AC-21**: 701–705, 1976.
9. J. H. Chow et al., *Time-Scale Modeling of Dynamic Networks with Applications to Power Systems,* Berlin: Springer-Verlag, 1982.
10. J. H. Chow et al., Inertial and slow coherency aggregation algorithms for power system dynamic model reduction, *IEEE Trans. Power Syst.,* **10**: 680–685, 1995.
11. H. K. Khalil, Output feedback control of linear two-time-scale systems, *IEEE Trans. Autom. Control,* **AC-32**: 784–792, 1987.
12. D. Naidu and A. Rao, *Singular Perturbation Analysis of Discrete Time Control Systems,* Lecture Notes in Mathematics, Berlin: Springer-Verlag, 1985.
13. H. K. Khalil, On the robustness of output feedback control methods to modeling errors, *IEEE Trans. Autom. Control,* **AC-28**: 524–528, 1983.
14. B. D. Riedle and P. V. Kokotovic, Integral manifold of slow adaptation, *IEEE Trans. Autom. Control,* **AC-31**: 316–323, 1986.
15. J. H. Chow and P. V. Kokotovic, A two-stage Lyapunov-Bellman feedback design of a class of nonlinear systems, *IEEE Trans. Autom. Control,* **AC-26**: 656–663, 1981.
16. Z. Pan and T. Basar, H^∞-optimal control for singularly perturbed systems, Part I: Perfect state measurements, *Automatica,* **29**: 401–423, 1993.
17. Z. Pan and T. Basar, H^∞-optimal control for singularly perturbed systems, Part II: Imperfect state measurements, *IEEE Trans. Autom. Control,* **39**: 280–299, 1994.
18. K. D. Young, P. V. Kokotovic, and V. I. Utkin, A singular perturbation analysis of high gain feedback systems, *IEEE Trans. Autom. Control,* **22**: 931–938, 1977.
19. A. J. Calise, Singular perturbation methods for variational problems in aircraft control, *IEEE Trans. Autom. Control,* **21**: 345–353, 1976.
20. H. J. Kelley, Aircraft maneuver optimization by reduced order approximations, In C. T. Leonides, (ed.), *Control and Dynamics Systems,* New York: Academic Press, 131–178, 1973.
21. F. Delebecque and J. P. Quadrat, Optimal control of Markov chains admitting strong and weak interactions, *Automatica,* **17**: 281–296, 1981.
22. G. Peponides and P. V. Kokotovic, Weak connections, time scales and aggregation of nonlinear systems, *IEEE Trans. Autom. Control,* **28**: 729–735, 1983.
23. H. K. Khalil, Feedback control of nonstandard singularly perturbed systems, *IEEE Trans. Autom. Control,* **34**: 1052–1060, 1989.
24. A. Bensoussan, Singular perturbation results for a class of stochastic control problems, *IEEE Trans. Autom. Control,* **26**: 1071–1080, 1981.
25. A. Bensoussan, J. L. Lions, and G. C. Papanicolaou, *Asymptotic Analysis for Periodic Structures,* New York: North-Holland, 1981.
26. V. A. Sobolev, Integral manifolds and decomposition of singularly perturbed systems, *Systems and Control Letters,* **5**: 169–179, 1984.
27. R. E. O'Malley, Jr., *Singular Perturbation Methods for Ordinary Differential Equations,* Berlin: Springer-Verlag, 1991.

PETAR V. KOKOTOVIC
University of California, Santa Barbara

JOE H. CHOW
Rensselaer Polytechnic Institute

HASSAN K. KHALIL
Michigan State University

SINUSOIDAL STEADY STATE. See NETWORK ANALYSIS, SINUSOIDAL STEADY STATE.